Hydro-Forming of U-Shaped Parts with Branches

Mai Thi Trinh
University of Economics – Technology for Industries, 456 Minh Khai, Vinh Tuy Ward, Hai Ba Trung District, Hanoi, Vietnam
ttmai@uneti.edu.vn

Trung Dac Nguyen
Hanoi University of Science and Technology, 1 Dai Co Viet, Bach Khoa ward, Hai Ba Trung district, Hanoi, Vietnam
trung.nguyendac@hust.edu.vn

Quoc Tuan Pham
Hanoi University of Science and Technology, 1 Dai Co Viet, Bach Khoa ward, Hai Ba Trung district, Hanoi, Vietnam
tuan.phamquoc@hust.edu.vn

Anh Ngoc Pham
School of Mechanical Engineering, Vietnam Maritime University, Hai Phong, Vietnam
anhphamdhhp@gmail.com

Duy Van Dinh
Hanoi University of Science and Technology, 1 Dai Co Viet, Bach Khoa ward, Hai Ba Trung district, Hanoi, Vietnam
duy.dinhvan@hust.edu.vn (corresponding author)

Received: 10 October 2024 | Revised: 31 October 2024 | Accepted: 16 November 2024

 DOI: https://doi.org/10.48084/etasr.9227

ABSTRACT

Tube parts formed by hydroforming technology have many outstanding advantages, such as high mechanical properties, fast forming time, and the ability to shape complex parts. U-shaped tube parts with branches are applied in various fields, such as the automotive, electronics, and medical industries. The current challenges in hydroforming technology for manufacturing these parts lie in controlling and determining suitable process parameters to ensure the highest product quality. Through numerical simulations and theoretical calculations, with the input material being a copper tube made from CDA110, this study has investigated the parameters of die cavity fluid pressure and punch displacement. Based on these results, a regression equation for the relationship between fluid pressure and punch displacement was established, which allows for determining the appropriate ranges for fluid pressure and punch displacement to successfully hydroform U-shaped parts with branches. The research results aim to assist engineers in reducing the time required to identify suitable process parameters for hydroforming similar-shaped parts.

Keywords-hydroforming; tube fitting; pressure processing; numerical simulation; U-bend tube with branch

I. INTRODUCTION

Hydroforming is an advanced manufacturing technology widely used in the automotive, aerospace, and medical industries due to its ability to shape complex parts with high precision and good surface quality [1]. This method allows the forming of products from sheet metal and tubes with uniform stress distribution, minimizing defects and improving the mechanical strength of the final product [1]. Many studies have addressed the influence of fluid pressure and axial feeding on the forming process of metal tubes [2-6]. These studies include the analysis of necking in the hydroforming process, the prediction of bursting failures, and the role of axial feeding in the forming process [2-4]. Some studies focus solely on the effect of fluid pressure without considering axial feeding [5, 7], while others highlight the relationship between axial feeding and tube formability [8, 9]. Although considerable research has been conducted on hydroforming for straight tubes, the application of this technology to pre-bent tubes, particularly U-shaped tubes, remains limited. Most current studies primarily focus on straight tubes or simple shapes [2, 6, 10-15]. The U-shaped tubes pose various challenges, including uneven stress distribution, the risk of unintended deformation, and the complexity of controlling the final shape. The objective of this study is to analyze the hydroforming process for annealed copper CDA110 tube billets with an initial U-shaped curvature. Specifically, the present study aims to:

- Conduct a numerical simulation of the THF process, using Abaqus/CAE software to build a simulation model for the hydroforming process, with boundary conditions set to closely replicate real-world production settings.
- Develop regression equations. Simulation data are collected to build regression equations for key variables such as thinning (B) at the farthest bulge, thickening (N) at the lowest point of the U-bend, and boss height (H_v).
- Carry out a result analysis, that is, an evaluation of the influence of input variables, such as the part's geometric dimensions, internal die fluid pressure P_i, and punch displacement A_c, on the final product's geometric variables.

This study not only expands the understanding of the hydroforming process for U-shaped tube billets, but also provides useful analytical tools for the design and optimization of the manufacturing process. The regression equations developed can serve as predictive tools to improve production quality and efficiency while reducing risks and production costs.

II. MATERIAL AND METHOD

A. Material and Billet Shape

The part is formed from a pre-bent U-shaped tube billet, with the geometric parameters shown in Figure 1. The material used is annealed Cu CDA110, and the/its properties are listed in Table I [11]. The initial U-shaped billet is assumed to have a uniform wall thickness of 0.81 mm across the entire U-shaped region, with no residual stress from previous operations.

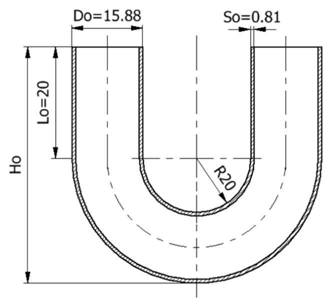

Fig. 1. U-shaped tube billet.

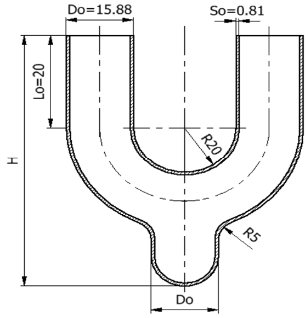

Fig. 2. Detail after forming.

TABLE I. TECHNICAL CHARACTERISTICS OF CU CDA110 MATERIAL AFTER ANNEALING [11]

Parameters and technical characteristics of CDA110 material	Value
Material parameter surveying temperature (°C)	24
Density, ρ(kg/m^3)	8940
Elastic modulus, E (GPa)	115
Material constants, C (MPa)	325
Endurance limit exponent, n	0.54
Poisson's ratio, v	0.33
Yield strength, σ_y (MPa)	170
Tensile strength, σ_u (MPa)	370
Relative elongation, ε (%)	40

B. Simulation Software

The present study utilizes the Abaqus/CAE software to conduct numerical simulations of the hydroforming process. Abaqus/CAE is a powerful tool for Finite Element Analysis (FEA), enabling accurate simulation of deformation and stress processes in materials [16].

1) Geometry and Finite Element Mesh Simulation

The geometric model of the U-shaped tube billet is constructed in the Abaqus/CAE software with the following specific dimensions, as depicted in Figure 1:

- Billet length: 65 mm
- Billet outer diameter: 15.88 mm
- Tube thickness: 0.81 mm
- Bend radius: 20 mm

To optimize the simulation time due to the symmetry of the part, only ¼ of the component is modeled. The billet is treated as a deformable body, while the die and punch are defined as rigid elements. The interactions between the billet, die, and punch are illustrated in Figure 3.

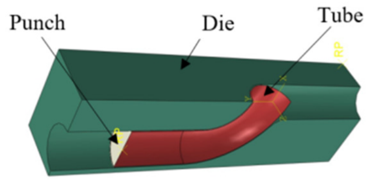

Fig. 3. Assembly model used for simulation in Abaqus/CAE.

Figure 4 shows that the finite element mesh is created using S4R tetrahedral elements, with a total of 1950 elements. This selection is made to ensure the accuracy of the simulation results while not excessively increasing the computation time for the tube.

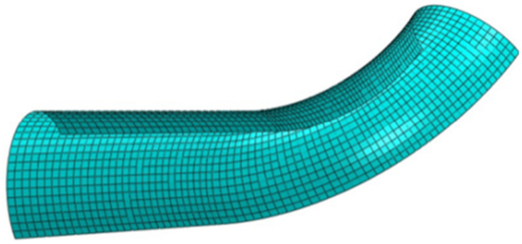

Fig. 4. Finite element mesh model of the tube component.

2) Boundary Conditions

The simulation is conducted under a friction coefficient of 0.1 for all positions with relative movement, while the billet and die cavity interact through contact throughout the forming simulation. The internal die cavity fluid pressure P_i is uniformly applied to the inner surface of the billet. The punch is moved at a fixed distance A_c along the axis of the billet. The outer surfaces of the billet are constrained to prevent free movement, ensuring an accurate simulation of the hydroforming process.

a) Calculation of the Fluid Pressure in the Die Cavity

Authors in [17] used the single-action THF method to determine the fluid pressure limit region. The internal pressure at the flow point is calculated by:

$$(P_i)_y = \sigma_y \frac{2S_0}{(D_0 - S_0)}$$

The maximum internal pressure can be calculated by [17]:

$$(P_i)_b = \sigma_u \frac{2S_0}{(D_0 - S_0)}$$

where:

$(P_i)_y$: Fluid pressure to reach the yield limit.

$(P_i)_b$: Fluid pressure to reach the ultimate limit.

σ_y: Yield strength (N/mm²).

σ_u: Ultimate tensile strength (N/mm²).

S_0: Initial tube wall thickness (mm).

D_0: Outer diameter of the tube (mm).

Applying this to copper CDA110 material, we obtain:

$$(P_i)_y = \sigma_y \frac{2S_0}{(D_0 - S_0)} = 170 \frac{2 \times 0.81}{15.88 - 0.81} = 18.27(\text{MPa})$$

$$(P_i)_b = \sigma_u \frac{2S_0}{(D_0 - S_0)} = 370 \frac{2 \times 0.81}{15.88 - 0.81} = 39.76(\text{MPa})$$

Therefore, when there is no axial displacement of the punch, the fluid pressure ranges from 18.27 MPa to 39.76 MPa. In the simulation of the hydroforming process, the axial displacement of the punch is considered. So, the fluid pressure range P_i from 20 MPa to 40 MPa in the die cavity was investigated. Specifically, P_i values of 20 MPa, 25 MPa, and 30 MPa are randomly selected for simulation.

b) Calculation of the Axial Displacement of the Punch

The punch displacement A_c is intended to compensate for the material in the formed branch. Hence, it largely depends on the material being studied and the specific objectives of different research. The punch displacement can be considered within various value ranges, and the resulting outcomes can be then evaluated. In this study, the investigated punch displacements A_c are 8 mm, 10 mm, and 12 mm.

3) Simulation Process

The hydroforming process is simulated by simultaneously applying fluid pressure P_i and punch displacement A_c. This process is carried out over a sufficiently long duration to ensure the stability of the simulation and to gather comprehensive data on deformation and stress within the billet. The fluid pressure P_i and punch displacement A_c are established, as shown in Figures 5-6.

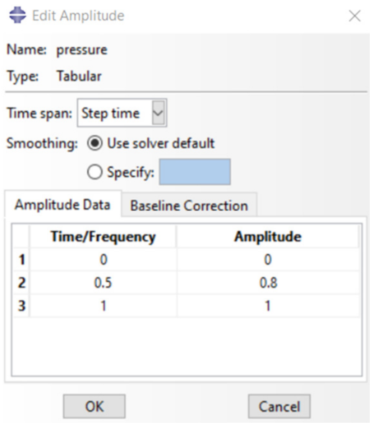

Fig. 5. Fluid pressure P_i amplitude as a function of time.

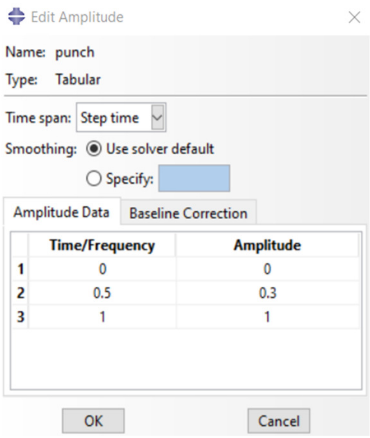

Fig. 6. Amplitude of punch displacement A_c over time.

4) *Results Collection and Data Analysis*

After performing the simulation, the results are obtained, as detailed in Figure 7.

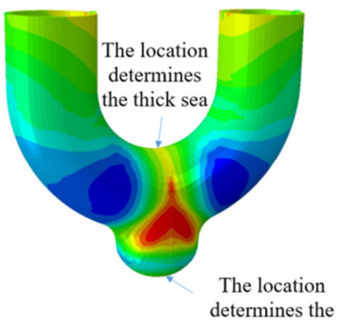

Fig. 7. Image of the product after hydroforming simulation in Abaqus/CAE.

The data from the simulations include the thinning variable B at the farthest bulge position, the thickening variable N at the lowest point of the U-bend, and the boss height H_v, as portrtayed in Table II. These values are then used to develop regression equations [18] deploying the least squares method.

5) *Building the Regression Equations*

The least squares method is employed to develop regression equations for the variables B, N, and H_v based on the input variables, which include, the geometric dimensions of the billet, the fluid pressure inside the mold cavity P_i, and the punch axial displacement A_c. These regression equations provide a predictive model to optimize the hydroforming process and control the quality of the final product. The regression equations take the following form:

The regression equation for the thickness variable of the part is:

$N = a_0 + a_1P_i + a_2A_c$ and $B = b_0 + b_1P_i + b_2A_c$.

The regression equation for the bunch height (H_v):

$H_v = c_0 + c_1P_i + c_2A_c$.

III. RESULTS AND DISCUSSION

After running the simulations and measuring the results, the parameters obtained are presented in Table II.

TABLE II. SUMMARY OF PARAMETERS AND RESULTS OBTAINED FROM THE HYDROFORMING SIMULATION OF THE TUBE IN ABAQUS/CAE

TT	P_i	A_c	Thinning value (B)	Thickness variable value (N)	Boss height H_v
1	20	8	0.68198	0.87279	4.5909
2	20	10	0.61305	0.86216	5.3713
3	20	12	0.49964	0.85437	6.1839
4	25	8	0.69037	0.892	5.3107
5	25	10	0.62716	0.88275	6.1571
6	25	12	0.52114	0.87345	7.1422
7	30	8	0.69783	0.91994	6.4477
8	30	10	0.63931	0.90628	7.301
9	30	12	0.53443	0.89685	8.3373

A. *Thickness Variable*

The thickness variable N at the lowest belly position of the U shows significant changes according to the input variables. Figure 8 shows the degree of thickness variable N changing when the variables P_i, and A_c change.

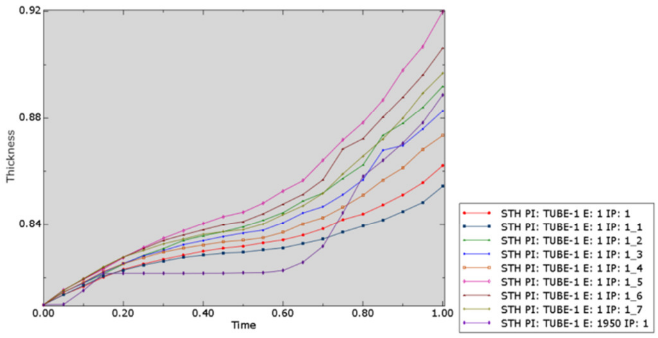

Fig. 8. Thickness variation over time under the effect of P_i (30 MPa) and A_c (10 mm) for element number 1.

Thickness equation by regression:

$$N = 0.8231 + 0.0045P_i - 0.0050A_c \quad (1)$$

This model can explain most of the variation in the thickness variable N value. When P_i increases, N increases, and when A_c increases, N decreases, which is not true for the hydrostatic stamping process, so the value of the N variable depends largely on the correlation between P_i and A_c, with the requirement that the thinning and thickening variables do not exceed 30%, the initial blank thickness is 0.81 mm. Then, (1) is only meaningful when:

$0.81\text{mm} < N < 1.053$ mm

$\Rightarrow 0.81 < N = 0.8231 + 00045P_i - 0.0050A_c < 1.053$

When the P_i value is between 20 MPa and 40 MPa then:

$10.2 \text{ mm} \leq A_c \leq 20.62$ mm

B. *Thinning*

The simulation results show that the thinning strain B at the farthest bulge position of the U-shaped tube blank strongly depends on the mold cavity fluid pressure P_i and the punch displacement A_c. Figure 9 illustrates the change of thinning strain B with different values of P_i and A_c.

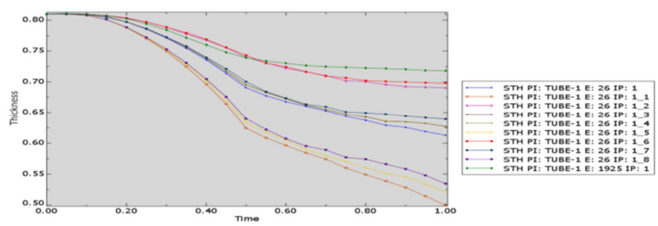

Fig. 9. Degree of thinning variation over time under the influence of P_i (30 MPa) and A_c (10 mm) for element number 26.

Thin variable equation is:

$$B = 0.9767 + 0.0026P_i - 0.0429A_c \quad (2)$$

When the P_i value is in the range from 20 MPa to 40 MPa then:

$$6.43 \text{ mm} \leq A_c \leq 10.76 \text{ mm}$$

1) Boss Height

Regression equation:

$$H_v = -3.0625 + 0.198P_i + 0.4428A_c \quad (3)$$

According to (3), H_v cannot have a negative value; thus, the H_v is maximized when both P_i and A_c are at their highest. Conversely, H_v reaches its minimum when the values of P_i and A_c are at their lowest limits. The results indicate that the boss height H_v increases with increasing pressure P_i and punch displacement A_c, or when either factor increases. To verify the accuracy of (1)-(3), further THF simulations were conducted, with A_c values being within the limit range. The measured and calculated values are presented in the chart in Figure 10.

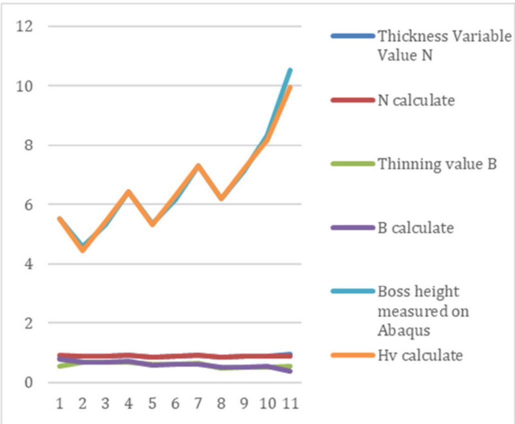

Fig. 10. Value chart of variables N, B, and H_v.

Figure 10 demonstrates that the alignment between the calculated results and those obtained from Abaqus software is nearly perfect, indicating that the reliability of (1)-(3) can be applied to both simulation and experimental studies. Equations (1) and (2) display that when P_i increases, both variables N and B respond accordingly, whereas they decrease when A_c decreases. These two variables are undesirable during the THF-forming process. However, if P_i increases without a corresponding increase in A_c, there will not be enough material to compensate for the boss region, leading to tearing at the largest bulge, as shown in Figure 11, and subsequently, Abaqus/CAE will report an error. When A_c increases significantly, the thickening region B is strongly compressed, causing the material to buckle, which creates folds, as depicted in Figure 12. Abaqus/CAE will also report an error when excessive deformation occurs. Therefore, the value of A_c needs to be aligned with the value of P_i to ensure that the boss has a shape that meets technical requirements. Hence, based on the results from (1) and (2), and the data collected from the simulations in Abaqus/CAE, the values of P_i and A_c are:

$$20 \text{ MPa} \leq P_i \leq 30 \text{ MPa}$$

$$6 \text{ mm} \leq A_c \leq 20 \text{ mm}$$

This is the range of Pi and Ac values that is best when shaping U-shaped curved pipe products.

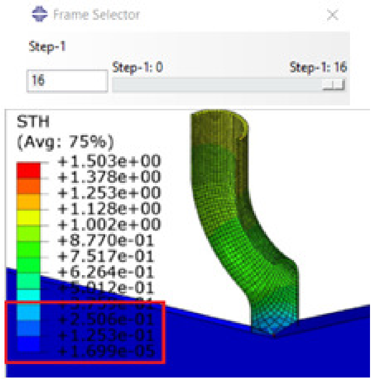

Fig. 11. The part is destroyed when P_i is large and A_c compensates the workpiece inappropriately.

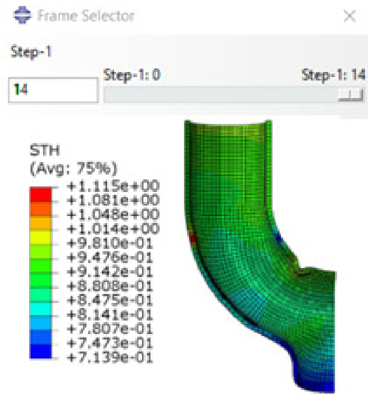

Fig. 12. The part is destroyed when P_i is small and A_c compensates for the large workpiece.

On the graph collected/formed from Abaqus/CAE, as seen in Figure 8, the purple line corresponds to P_i = 20 MPa, the punch displacement A_c = 8 mm, clearly showing that the thickness change is relatively sudden, and in contrast to other graph lines, it is quite smooth.

IV. CONCLUSIONS

The above study provides insights into the THF process for U-shaped curved tube billets, representing a unique investigation that has not been extensively researched before. It is observed that the numerical simulation method and the developed regression equations can contribute significantly to the optimization of the manufacturing process for this type of billet. The simulation results offer valuable insights into the behavior of materials under hydroforming conditions and help in developing regression equations for key deformations, such as thinning (B), thickening (N), and boss height (H_v). These findings improve the manufacturing process of U-shaped curved tubes, thereby enhancing product efficiency and quality. The current research opens opportunities for applying the results in industries that require the production of complex-shaped parts, such as the automotive and aerospace industries. The limitation of this study is that it focuses on a specific type of material and billet shape. Therefore, the results may not be fully applicable to other materials or shapes. Consequently, further research is needed on different materials and various billet shapes. Combining numerical simulations with practical experiments will help verify and improve the accuracy of the regression models. Additionally, the research can be expanded to include practical applications in industry.

REFERENCES

[1] N. V. Pham, *Hydraulic Stamping Technology*. Hanoi University of Science and Technology, 2006.

[2] R. Hashemi, "Analysis of necking in tube hydroforming by means of extended forming limit stress diagram," *Engineering Solid Mechanics*, vol. 2, no. 2, pp. 73–82, 2014.

[3] S.-W. Kim, W.-J. Song, B.-S. Kang, and J. Kim, "Bursting failure prediction in tube hydroforming using FLSD," *The International Journal of Advanced Manufacturing Technology*, vol. 41, no. 3, pp. 311–322, Mar. 2009, https://doi.org/10.1007/s00170-008-1488-3.

[4] V. Paunoiu, O. Ciocan, and D. Nicoara, "Numerical Study of Tube Hydroforming Technology," *International Journal of Modern Manufacturing Technologies*, vol. 2, no. 1, pp. 67–72, May 2010.

[5] R. Kant and D. Kumar, "Effect of Die Entrance Radius on Tube Formability in Closed-Die Tube Hydroforming," *International Journal of Applied Science & Technology Research Excellence*, vol. 1, no. 1, pp. 1–6, Dec. 2011.

[6] M. Imaninejad, G. Subhash, and A. Loukus, "Loading path optimization of tube hydroforming process," *International Journal of Machine Tools and Manufacture*, vol. 45, no. 12–13, pp. 1504–1514, Oct. 2005, https://doi.org/10.1016/j.ijmachtools.2005.01.029.

[7] J. P. Abrantes, A. Szabo-Ponce, and G. F. Batalha, "Experimental and numerical simulation of tube hydroforming (THF)," *Journal of Materials Processing Technology*, vol. 164–165, pp. 1140–1147, May 2005, https://doi.org/10.1016/j.jmatprotec.2005.02.117.

[8] B. G. Marlapalle and R. S. Hingole, "Predictions of formability parameters in tube hydroforming process," *SN Applied Sciences*, vol. 3, no. 6, May 2021, Art. no. 606, https://doi.org/10.1007/s42452-021-04533-4.

[9] B. Sreenivasulu, G. Prasanthi, T. Naresh Kumar, "Vimulative analysis of tube hydroforming process," *International Journal of Research in Engineering and Technology*, 2013, pp. 756-763.

[10] N. Asnafi, "Analytical modelling of tube hydroforming," *Thin-Walled Structures*, vol. 34, no. 4, pp. 295–330, Aug. 1999, https://doi.org/10.1016/S0263-8231(99)00018-X.

[11] Q. D. Vu, T. D. Nguyen, H. V. Dang, and D. T. Phan, "Effect of loading paths on hydroforming ability of stepped hollow shaft components from double layer pipes," *EUREKA: Physics and Engineering*, no. 4, pp. 143–154, Jul. 2023, https://doi.org/10.21303/2461-4262.2023.002797.

[12] M. Kazeminezhad, *Metal Forming: Process, Tools, Design*. BoD – Books on Demand, 2012.

[13] M. Kadkhodayan, A. Erfani Moghadam, and M. Heidari, "Loading path optimization of T-shape tube hydroforming process," *Steel Research International*, vol. 81, no. 9, Jan. 2010.

[14] H. Sadłowska and A. Kocańda, "On the problem of material properties in numerical simulation of tube hydroforming," *Archives of Civil and Mechanical Engineering*, vol. 10, no. 4, pp. 77–83, Dec. 2010, https://doi.org/10.1016/S1644-9665(12)60033-8.

[15] M.-T. Nguyen, T.-H. Tran, D.-D. Le, D.-T. Tran, D.-T. Bui, and B. T. Anh, "The Influence of Capillary Geometry on the Stiffness of Hydrostatic Bearings in Medium-Sized Cylindrical Grinding Machines: A Simulation Analysis," *Engineering, Technology & Applied Science Research*, vol. 14, no. 4, pp. 15993–15999, Aug. 2024, https://doi.org/10.48084/etasr.7976.

[16] Simulia, *"Abaqus 2016 Documentation,"* [Online]. Available: http://130.149.89.49:2080/v2016/index.html.

[17] K. N. Bogoyavlensky *et al.*, *Hydroplastic treatment of metals*. 1988.

[18] A. T. Nguyen, G. D. Lai, and H. D. Tran, *Textbook on Experimental Design and Data Processing in Engineering.* Hanoi, Vietnam: People's Army Publishing House, 2019.